Local topological switch for boundary states in quantum walks

Xiang Zhan [1], Yue Yu, [1] and Peng Xue [2,*]
[1] *School of Physics and MIIT Key Laboratory of Semiconductor Microstructure and Quantum Sensing, Nanjing University of Science and Technology, Nanjing 210094, China*
[2] *Beijing Computational Science Research Center, Beijing 100084, China*

(Received 19 July 2023; accepted 13 December 2023; published 4 January 2024)

Localization is a critical phenomenon in quantum walks that has attracted much attention in quantum simulations. In this paper, we present a unified framework for investigating the localization due to two causes, single-position defects and topology. Furthermore, we show that a specific phase defect can act as a topological switch, which can turn on (off) topological boundary states between two regions with the same (different) topological numbers. Remarkably, the localized state turned on by the switch is protected by topological features. Thus, the switch is a topologically nontrivial defect that significantly differs from ordinary defects. Our results provide new intuitive insight into the topological features of quantum walks and shed new light on manipulating quantum walks.

DOI: 10.1103/PhysRevA.109.012409

I. INTRODUCTION

Quantum walks (QWs) provide a powerful and versatile platform for quantum information processing [1–10]. As the quantum analogy of classical random walks, QWs describe the evolution of a quantum particle (walker) on a lattice. One key characteristic of a QW is the ballistic behavior of the spreading of the walker [11,12], which has inspired its successful use in accelerating the resolution of search problems [13–18]. In contrast to ballistic spreading, it is possible to trap the walker in specific locations through properly engineering [19–28], which plays a vital role in quantum simulations based on QWs [29–36]. Recently, quantum simulation based on QWs, as a state-of-art technique, has provided a powerful way to explore topological phenomena [37–46].

There are intriguing connections between topology and disorder, an important cause of localization inspired by Anderson localization [35,36,47–52]. On one hand, introducing topology can suppress the localization caused by the static disorder, resulting in the phenomenon known as topological Anderson localization transition [53,54]. On the other hand, topological boundary states are robust against disorder [55]. However, it remains an open question as to what the relationship is between localizations caused by single-position defects [56–60] and nontrivial topological boundaries.

Intuitively, single-position defects and nontrivial topological boundaries are two completely distinct causes of localization. This is because defects typically activate localization in homogeneous QWs, where coin operations on either side of the position are the same. On the contrary, a topological boundary state appears at the nontrivial topological boundary of which the two sides have different topological numbers.

In this paper, we investigate the localization at a certain position through an intuitive way that combines localization states on either side of the position. The coin operation at that position determines which localized states can be combined. This approach provides a unified framework for investigating localizations caused by single-position defects and topology. Based on this approach, we explore the effects of defects on topological boundary states. Notably, we introduce a specific phase defect that can deterministically activate topological edge states at the boundary between two regions with the same topological number. This phase defect also has the potential to eliminate conventional topological boundary states, providing a topological switch for the boundary state. Interestingly, the activated localized state is ensured and protected by topological features in the same manner as the conventional topological boundary state. Therefore, the switch is a topologically nontrivial defect that is significantly different from ordinary defects.

This paper is organized as follows. In Sec. II, we introduce a feature of the eigenstates of QWs. Based on this feature, we introduce our method to obtain these eigenstates in Sec. III. In Sec. IV, we present our main results of switching on and off the topological boundary state. Finally, we summarize our work in Sec. V.

II. SPLIT-STEP QW

In a one-dimensional discrete-time QW, the basis of the walker is $|x,\delta\rangle = |x\rangle \otimes |\delta\rangle$, which is composed of the position state $|x\rangle$ for $x \in \mathbb{Z}$ and the coin state $|\delta\rangle$ for $\delta \in \{\pm 1\}$. The dynamics of the QW are governed by iteratively implementing the coin-flipping operation $C = \sum_{x\in\mathbb{Z}} |x\rangle\langle x| \otimes C_x$ followed by the conditional shift operation $S = \sum_{x\in\mathbb{Z},\delta=\pm 1} |x+\delta\rangle\langle x| \otimes |\delta\rangle\langle\delta|$, where $C_x \in \mathrm{SU}(2)$ is the coin operation at the position x.

In this paper, we consider the split-step QW, where each step comprises two iterations of the coin and shift operations,

*gnep.eux@gmail.com

resulting in the step operation of each step as $W = SCSC$. In this case, the walker only appears at even positions after each step when it starts at even positions. Starting with an initial state $|\Psi_0\rangle$, the state after step t is $|\Psi_t\rangle = W^t |\Psi_0\rangle$.

In the following, let us consider a particular property of eigenstates $|\psi\rangle$ of the QW operator W. According to the eigenequation $W|\psi\rangle = \lambda|\psi\rangle$ with eigenvalues $\lambda \in \{\mathbb{C} : \|\lambda\| = 1\}$, it is easy to have the following equality between two probabilities: $\| \langle x, -\delta\rangle \psi\|^2 + \sum_{x'\in(\mathbb{Z}_\delta+\delta x)} \|\langle x'\rangle \psi\|^2 = \|\langle x, -\delta| W|\psi\rangle\|^2 + \sum_{x'\in(\mathbb{Z}_\delta+\delta x)} \|\langle x'| W|\psi\rangle\|^2$ for arbitrary x and δ, where $\langle x|$ is a simplification of $\langle x| \otimes \mathbb{1}_c$ with $\mathbb{1}_c$ being the identity operator of coin space. Substituting the operator W, the probability on the right-hand side can be further deduced into $\|\langle x, \delta| C|\psi\rangle\|^2 + \sum_{x'\in\mathbb{Z}_+} \|\langle x' + \delta x| |\psi\rangle\|^2$, which implies $\|\langle x, -\delta| |\psi\rangle\|^2 = \|\langle x, \delta| C|\psi\rangle\|^2$. Therefore, for any eigenstate $|\psi\rangle$, the action of coin operation C_x on the coin state $|\psi_x\rangle = \langle x\rangle \psi$ at the position x is equivalent to the action of a new coin operation as

$$X(\omega_+, \omega_-) = \textstyle\sum_{\delta=\pm} \omega_\delta |\delta\rangle\langle -\delta|, \tag{1}$$

which is an inversion operation with certain additional phases $\omega_\delta \in \{\mathbb{C} : \|\omega_\delta\| = 1\}$. In other words, an eigenstate $|\psi\rangle$ of a QW is also an eigenstate of a new QW with coin operation C_x at the position x being changed to $X(\omega_+, \omega_-)$.

Without loss of generality, let us separate the eigenstate $|\psi\rangle$ into two parts as

$$|\psi\rangle = \alpha_+ |\psi_+\rangle + \alpha_- |\psi_-\rangle, \tag{2}$$

where $\|\alpha_+\|^2 + \|\alpha_-\|^2 = 1$, $\| |\psi_+\rangle \| = \| |\psi_-\rangle \| = 1$, and $\alpha_\epsilon |\psi_\epsilon\rangle$ is the part of $|\psi\rangle$ corresponding to a side of the position 0 with $\langle x, \delta| \alpha_\epsilon |\psi_\epsilon\rangle = \langle x, \delta\rangle \psi$ for $(x \in \mathbb{Z}_\epsilon \wedge \delta = \pm) \vee (x = 0 \wedge \delta = -\epsilon)$, and $\langle x, \delta| \alpha_\epsilon |\psi_\epsilon\rangle = 0$ otherwise. This state is also an eigenstate of the new QW with coin operation $C_{x=0}$ at position 0 being changed to $X(\omega_+, \omega_-)$. In the new QW, the coin operation $X(\omega_+, \omega_-)$ makes position 0 a reflecting boundary with additional reflecting phases (ω_+, ω_-), which means a walker on either side of the boundary cannot walk to the other side. This new QW is equivalent to two independent QW on half lines (QWHLs) [61]. For each QWHL, the eigenstates $|\psi_\epsilon\rangle$ depend only on coin operations C_x on the half line, with $x \in \mathbb{Z}_\epsilon$ and the reflecting phase ω_ϵ. Therefore, an arbitrary eigenstate of a QW can be separated into two eigenstates of two QWHLs.

III. OBTAINING EIGENSTATES VIA PHASE MATCHING

Given a pair of eigenstates $(|\psi_+(\omega_+)\rangle, |\psi_-(\omega_-)\rangle)$ of two QWHLs with reflecting phases (ω_+, ω_-), one can combine them to obtain an eigenstate of the QW with coin operation C_0 at position 0 if and only if the following two conditions hold: (i) The eigenvalues corresponding to the pair of eigenstates are identical as $\lambda_+(\omega_+) = \lambda_-(\omega_-)$; (ii) there is a pair of α_ϵ so that

$$C_0 \begin{pmatrix} \alpha_- \langle 0, +1\rangle \psi_- \\ \alpha_+ \langle 0, -1\rangle \psi_+ \end{pmatrix} = \begin{pmatrix} \omega_+ \alpha_+ \langle 0, -1\rangle \psi_+ \\ \omega_- \alpha_- \langle 0, +1\rangle \psi_- \end{pmatrix}. \tag{3}$$

When these two conditions are satisfied, the combined eigenstate of the QW is $|\psi\rangle = \alpha_+ |\psi_+\rangle + \alpha_- |\psi_-\rangle$ and the corresponding eigenvalue is $\lambda = \lambda_+(\omega_+) = \lambda_-(\omega_-)$.

For a given coin operation C_0, condition (ii) is equivalent to that $X(\omega_+, \omega_-)C_0$ has an eigenvalue as 1. Therefore, this condition is a phase-matching condition determined by the two reflecting phases ω_+ and ω_-. For example, let us consider $C_0 = C^{\mathrm{I}}(\theta_0)$ in a widely used type of coin operation as $C^{\mathrm{I}}(\theta) = e^{-i\sigma_y\theta}$, where σ_y is the Pauli operator. Substituting this C_0 into Eq. (3) yields

$$\frac{\alpha_- \langle 0, +1\rangle \psi_-}{\alpha_+ \langle 0, -1\rangle \psi_+} = \frac{\omega_+ + s_0}{c_0} = \frac{c_0}{\omega_- - s_0}, \tag{4}$$

for $c_0 s_0 \neq 0$, where $c_0 = \cos\theta_0$ and $s_0 = \sin\theta_0$. The second equality of Eq. (4) is a phase-matching condition as $\omega_-(\omega_+) = \frac{1+s_0\omega_+}{\omega_+ + s_0}$. When this condition is saturated, there must be a pair of α_ϵ that can be directly calculated according to Eq. (4). For $c_0 = 0$ ($s_0 = 0$), the coin operation is $X(-1, 1)$ ($\mathbb{1}_c$) and the phase-matching condition is $\omega_+ = -\omega_- = \pm 1$ ($\omega_- = 1/\omega_+$).

Example: Conventional topological QW. As shown in Fig. 1(a), let us consider that the conventional topological QW with coin operations takes the form $C_x = C^{\mathrm{I}}(\theta_x)$ and the coin parameters are the same for odd (even) positions within each side, that is, $\theta_{\epsilon(2x-1)} = \theta_{\epsilon 1}$ and $\theta_{\epsilon 2x} = \theta_{\epsilon 2}$ for $x \in \mathbb{Z}_+$ and $\epsilon = \pm$. In this case, for each QWHL with reflecting phase ω_ϵ, it is not difficult to analytically obtain the eigenvalues and eigenstates (see the Appendix for details). For each QWHL with phase ω_ϵ, there exist two eigenstates that have the potential to be localized at position 0 with corresponding eigenvalues as

$$\lambda_\epsilon^\varepsilon = \omega_\epsilon \frac{i\epsilon s_{\epsilon 1}\mathrm{Im}(\omega_\epsilon) + \varepsilon\sqrt{[\epsilon s_{\epsilon 2} + \mathrm{Re}(\omega_\epsilon)]^2 + \mathrm{Im}(\omega_\epsilon)^2 c_{\epsilon 1}^2}}{\epsilon s_{\epsilon 2} + \omega_\epsilon}, \tag{5}$$

where $\varepsilon = \pm 1$ comes from the quadratic formula. Each eigenvalue λ_ϵ corresponds to an eigenstate as

$$|\psi_\epsilon\rangle = \beta_{0,-\epsilon} |0, -\epsilon\rangle + \sum_{n\in\mathbb{Z}_+} \sum_{\delta'=\pm} \beta_{\epsilon n,\delta'} |\epsilon 2n, \delta'\rangle, \tag{6}$$

where

$$\begin{aligned} \beta_{\epsilon n,+} &= Az^n, n \in \mathbb{Z}_+, \\ \beta_{\epsilon n,-} &= \frac{c_{\epsilon 2} - c_{\epsilon 1}\lambda_\epsilon z}{\epsilon s_{\epsilon 2} + \epsilon s_{\epsilon 1}\lambda_\epsilon} Az^n, n \in \mathbb{Z}_+, \\ \beta_{0,-\epsilon} &= \frac{c_{\epsilon 1}\lambda_\epsilon}{\omega_\epsilon - \epsilon s_{\epsilon 1}\lambda_\epsilon} Az, \end{aligned} \tag{7}$$

$z = \frac{c_{\epsilon 2}(\omega_\epsilon - \epsilon s_{\epsilon 1}\lambda_\epsilon)}{c_{\epsilon 1}\lambda_\epsilon(\omega_\epsilon + \epsilon s_{\epsilon 2})}$, and A is the normalization factor. When the stationary constraint $\|z\| < 1$ is saturated, the eigenstate has a nonzero probability at position 0.

Considering the coin operation $C_0 = C^{\mathrm{I}}(\theta_0)$, the stationary eigenstates $|\psi\rangle$ are obtained through combining state $|\psi_\pm\rangle$ in Eq. (6) as follows. First, for each ω_+, there is only one matching phase of ω_- given by $\omega_-(\omega_+)$ that is determined by C_0. Therefore, we have spectrums of two QWHLs $\lambda_+(\omega_+)$ and $\lambda_-[\omega_-(\omega_+)]$ with respect to the phase ω_+, as shown in the left column of Fig. 1(c). Solving the equation $\lambda_+(\omega_+) = \lambda_-[\omega_-(\omega_+)]$ with the variable ω_+ gives identical eigenvalues that satisfy the phase-matching condition. Among these

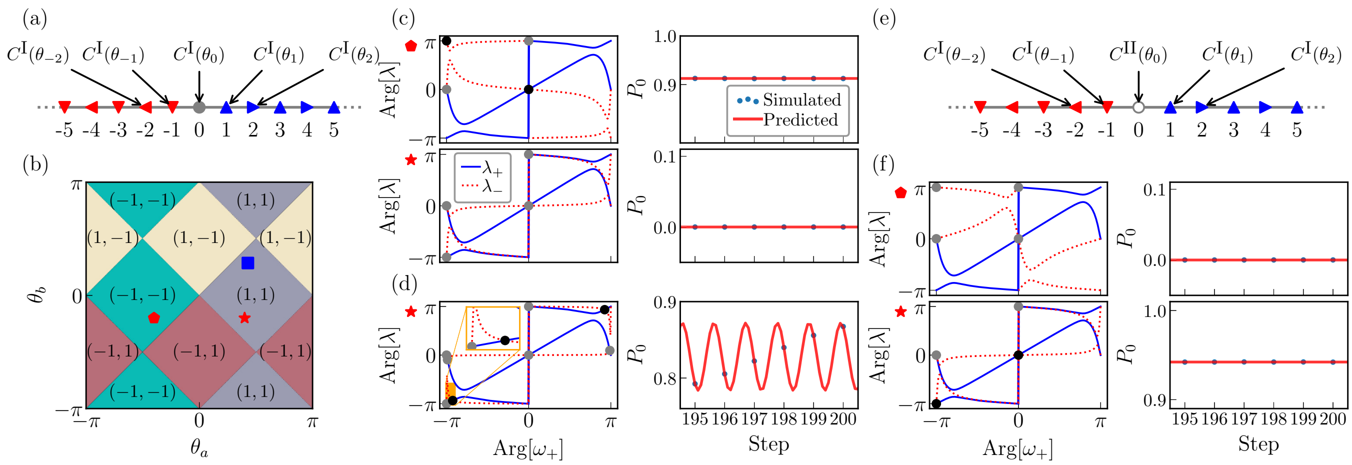

FIG. 1. Results of topological QWs. (a) Settings of coin operations for a conventional topological QW. (b) Diagram of phases $(\omega_+^+, -\omega_+^-)$ for (θ_1, θ_2) take the values (θ_a, θ_b). The blue square denotes the choice of (θ_1, θ_2). The red pentagon and star denote two choices of $(\theta_{-1}, \theta_{-2})$. (c) Results of conventional topological QWs with $\theta_0 = \theta_2$. The upper (lower) row shows that these are (not) a topological boundary state at 0 when the left region has a different (the same) topological number with the right region. (d) Ordinary defect as $\theta_0 = \theta_1$ activates localization with other coin operations, the same as the lower row of (c). (e) Settings of coin operations with a local switch $C^{\mathrm{II}}(\theta_0)$ in conventional topological QW. (f) Upper (lower): Switch off (on) boundary state with the local switch compared to the upper (lower) row of (c). In (c), (d), and (f), the left figures show the eigenvalues λ_+ (blue) and λ_- (red) vs the phase ω_+, and the right figures show the probabilities of the walker at 0.

obtained eigenvalues, we only keep these with localized eigenstates by checking the stationary condition $\|z\| < 1$.

After obtaining all localized eigenstates $|\psi_j\rangle$ and the corresponding eigenvalues λ_j with $j = 1, \ldots, m$, one can predict the probability distributions of the walker. For an initial state $|\Psi_0\rangle$ distributed in a finite number of positions near x, the probability of finding the walker at position x after many steps $t \gg x$ is given by

$$P(x, t) = \sum_{\delta=\pm} \left\| \sum_{j=1}^{m} \lambda_j^t \langle \psi_j \rangle \Psi_0 \langle x, \delta \rangle \psi_j \right\|^2. \tag{8}$$

The probabilities P_0 at position 0 for two typical cases of topological QWs are shown in the right column of Fig. 1(c). Moreover, we introduce a coin defect to 0 of the topological QW without a boundary state and obtain a localization at 0, as shown in Fig. 1(d). These results straightforwardly show that the probability in Eq. (8) precisely predicts the behaviors of the walker at position 0. We will further discuss these results later.

IV. CONNECTION TO TOPOLOGICAL THEORY

A. Topological numbers

As shown in Fig. 1(c), the probabilities at position 0 perfectly align with the qualitative predictions of the topological theory, that is, a boundary state must appear at the boundary between two regions with different topological numbers. In the following, we delve deeper into the relationship between our method and topological theory.

First, let us consider the QWHL on the right side of position 0 with reflecting phase ω_+. According to Eq. (A14), two extreme eigenvalues $\lambda_+ = \pm 1$ can be obtained when and only when the reflecting phase is $\omega_+ \in \{\pm 1\}$. Further taking into account the stationary condition $\|z\| < 1$, each extreme eigenvalue $\lambda_+ \in \{\pm 1\}$ can be obtained by one and only one specific phase, which we denote as $\omega_+^{\lambda_+} \in \{\pm 1\}$. The pair of phases $(\omega_+^+, -\omega_+^-)$ for different coin parameters (θ_1, θ_2) are illustrated in Fig. 1(b). It is interesting that this pair of phases is invariant for (θ_1, θ_2) within a certain region, which is equivalent to the pair of topological numbers [55] of the QW with coin operations $C_{2x} = C^{\mathrm{I}}(\theta_2)$ and $C_{2x+1} = C^{\mathrm{I}}(\theta_1)$ for $x \in \mathbb{Z}$.

Next, let us consider the case (C1) where the left and right regions have a different topological number, as shown in the first row of Fig. 1(c). According to the equivalence relation between phases $(\omega_+^+, -\omega_+^-)$ and topological numbers, this case means that there is at least one extremal eigenvalue $\lambda \in \{\pm 1\}$ so that $\omega_+^{\lambda}(\theta_1, \theta_2) = -\omega_+^{\lambda}(\theta_{-1}, \theta_{-2})$. For the QWHL on the left, we also have that each extreme eigenvalue $\lambda_- \in \{\pm 1\}$ can be obtained by one and only one phase, $\omega_-^{\lambda_-} \in \{\pm 1\}$. In addition, this phase satisfies $\omega_-^{\pm}(\theta_{-1}, \theta_{-2}) = \omega_+^{\pm}(-\theta_{-1}, -\theta_{-2}) = -\omega_+^{\pm}(\theta_{-1}, \theta_{-2})$. Therefore, in the case (C1), a common eigenvalue λ of the two sides can be obtained by the same phase, $\omega_+^{\lambda}(\theta_1, \theta_2) = \omega_-^{\lambda}(\theta_{-1}, \theta_{-2}) \in \{\pm 1\}$. Whether this equivalent phase is 1 or -1, the phase-matching condition in Eq. (4) for $C_0 = C^{\mathrm{I}}(\theta_0)$ can always be satisfied for arbitrary θ_0. Thus, there must be a localized state at position 0, which provides an intuitive explanation of the topological boundary states predicted by the topological theory.

Finally, let us consider the other case (C2) where both topological numbers are the same for the left and right regions. In this case, we have $\omega_+^{\lambda}(\theta_1, \theta_2) = -\omega_+^{\lambda}(\theta_{-1}, \theta_{-2})$ for $\lambda = \pm 1$, as shown in the second row of Fig. 1(c). Therefore, each extremal eigenvalue $\lambda = \pm 1$ corresponds to different phases on the two sides $\omega_+^{\lambda} = -\omega_-^{\lambda} \in \{\pm 1\}$, which cannot satisfy the phase-matching condition given by Eq. (4) for $C_0 = C^{\mathrm{I}}(\theta_0)$. Hence, it is not ensured to have a boundary state at position 0. It is worth mentioning that a localized state may still occur by an appropriate coin parameter θ_0. As shown in Fig. 1(d), we change the coin parameter from $\theta_0 = \theta_2$ into $\theta_0 = \theta_1$ and obtain a localized state due to the coin defect.

B. Switch on and off the boundary state

In the discussion above, the generation of a conventional topological boundary state is ensured by the coin operation $C_0 = C^{\mathrm{I}}(\theta_0)$ always allowing the matching of identical extremal phases $\omega_+ = \omega_- \in \{\pm 1\}$. When both topological numbers of the two sides are the same, a straightforward idea to obtain the boundary state is to choose a coin operation that always allows the matching of opposite phases, $\omega_+ = -\omega_- \in \{\pm 1\}$.

Here we consider another type of coin operation as $C_0 = C^{\mathrm{II}}(\theta_0)$ with $C^{\mathrm{II}}(\theta) = \sigma_z e^{i\sigma_y \theta}$. Substituting this coin operation into Eq. (3), we have the phase-matching condition as

$$\frac{\alpha_- \langle 0, +1 \rangle \psi_-}{\alpha_+ \langle 0, +1 \rangle \psi_-} = \frac{\omega_+ - s_0}{c_0} = \frac{c_0}{s_0 - \omega_-}, \tag{9}$$

for $c_0 s_0 \neq 0$. It is worth mentioning that this type of coin operation $C^{\mathrm{II}}(\theta)$ is equivalent to a phase defect σ_z of the coin operation $C^{\mathrm{I}}(-\theta)$.

It is easy to see that opposite phases $\omega_+ = -\omega_- \in \{\pm 1\}$ always satisfy the phase-matching condition given by Eq. (9) of $C^{\mathrm{II}}(\theta_0)$ for arbitrary θ_0. Therefore, using this type of coin operation at 0 [see Fig. 1(e)], there must be a boundary state at 0 for the case (C2). As an example, we choose coin operations that are the same as that in the second row of Fig. 1(c), but change the coin operation C_0 from $C^{\mathrm{I}}(\theta_0)$ into $C^{\mathrm{II}}(\theta_0)$. The result is shown in the second row of Fig. 1(f), where a boundary state is switched on compared to the result in the lower row of Fig. 1(c). We will show that this boundary state is significantly different from the localization due to the ordinary defect, as shown in Fig. 1(d).

On the other hand, the phases $\omega_+ = \omega_- \in \{\pm 1\}$ do not meet the phase-matching condition given by Eq. (9). Therefore, the coin operation $C_0 = C^{\mathrm{II}}(\theta_0)$ is possible to switch off the boundary state. An example is shown in the upper row of Fig. 1(f), where the coin operations are the same as that in the upper row of Fig. 1(c), but C_0 is changed to $C^{\mathrm{II}}(\theta_0)$ with $\theta_0 = -\theta_2$. It is to be noted that to switch off the boundary state, one should appropriately choose θ_0 to avoid the localization due to ordinary defects.

It is worth mentioning that for the case in which the two regions have a different and an identical topological number, e.g., $\omega_+^+(\theta_1, \theta_2) = \omega_+^+(\theta_{-1}, \theta_{-2})$ and $\omega_+^-(\theta_1, \theta_2) = -\omega_+^-(\theta_{-1}, \theta_{-2})$, both types of coin operations, $C^{\mathrm{I}}(\theta_0)$ and $C^{\mathrm{II}}(\theta_0)$, allow a boundary state at 0. To switch off this topological boundary state, the coin operation C_0 is necessary to have complex elements.

C. The switch is a topologically nontrivial defect

Although the switch is a defect, it is significantly different from ordinary defects. As discussed above, when the coin operation at 0 is a switch $C^{\mathrm{II}}(\theta_0)$, a localized state must exist when the two sides have a same topological number. However, the localization induced by ordinary defects is irrelevant of topological features. Therefore, the switch is a topologically nontrivial defect.

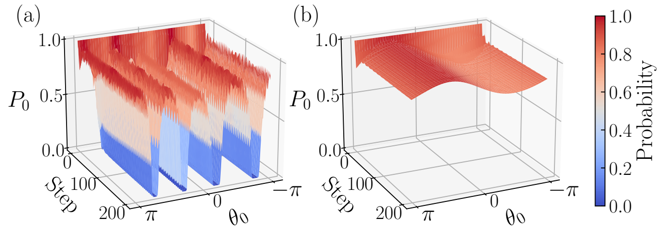

FIG. 2. Probabilities P_0 for different values of θ_0. The coin operation at 0 is (a) $C^{\mathrm{I}}(\theta_0)$ or (b) $C^{\mathrm{II}}(\theta_0)$, and coin operations at other positions are the same as those of the second row of Fig. 1(c).

From the perspective of phase matching, the switch matches extremal phases ± 1, which are in correspondence with topological numbers. Moreover, this phase matching is independent of θ_0 and specific coin operations in other positions. Similarly, this is the same as the phase matching for localization in conventional topological QWs. Conversely, for ordinary defects that are topologically trivial, the matched phases depend on θ_0 and coin operations of other positions. Thus, for these two different defects, we can see a significant difference between P_0 when changing θ_0 (see Fig. 2).

A key feature of topological boundary states is their robustness against disorders. It is worth noting that the localization due to a topologically trivial defect is also robust to disorders. In Fig. 3, we show the simulated behaviors of different localization states under disorders that depend on both position and step. In each simulation, the coin parameter at the position x and step t is randomly chosen as $\tilde{\theta}_x^t$ that follows a Gaussian distribution with a mean of θ_x and standard deviation σ. As shown in Fig. 3, there is no significant difference in robustness between topological boundary states and the localized state due to topologically trivial defects. Therefore, it is not enough to demonstrate that a localized state is a topological boundary state by observing its robustness against disorder. Our result

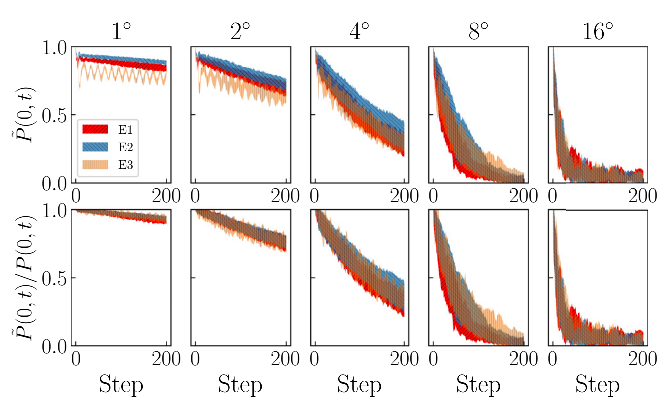

FIG. 3. Regions of probabilities $\tilde{P}(0, t)$ (upper row) and relative probabilities $\tilde{P}(0, t)/P(0, t)$ (lower row) within one standard deviation obtained from 20 simulations. Here, (E1), (E2), and (E3) correspond to the conventional topological boundary state in the first row of Fig. 1(c), the topological boundary state turned on by our switch in the second row of Fig. 1(f), and the localized state due to an ordinary defect in Fig. 1(d), respectively. Different columns correspond to strengths of disorder $\sigma = 1^\circ, 2^\circ, 4^\circ, 8^\circ, 16^\circ$.

suggests that observing its robustness against the coin defect might be a suitable choice.

V. CONCLUSION

In summary, we propose a method to obtain the eigenstates of a QW on a line by separating the line into two half lines and combining the eigenstates of two QWHLs. In our method, each QWHL has a phase-carrying reflection boundary, and the coin operation connecting the two half lines determines a matching condition for the two reflection phases. Interestingly, we reveal a correspondence between two specific reflection phases of a QWHL and the two topological numbers of the corresponding QW on a line. Based on these, we rigorously and quantitatively explain the mechanisms for the generation of topological boundary states and localized states caused by single-position defects. Furthermore, we propose a specific topological defect that can switch topological boundary states on and off. Our method provides a unified framework for localizations due to topology and single-position defects and exhibits their differences. Our work provides new insight into the topological properties of QWs and sheds new light on manipulating a QW. An important question that arises is whether our method can be applied to real materials. This would be an interesting issue to investigate in the future.

ACKNOWLEDGMENT

This work has been supported by the National Natural Science Foundation of China (Grants No. 92265209, No. 12025401, and No. 12004184).

APPENDIX: EIGENSTATES OF QWHL

Here, we give a detailed solution to the localized eigenstate of the QWHL with a reflecting phase ω_ϵ and coin operations $C_{\epsilon(2x-1)} = C_{\epsilon 1} = C^I(\theta_{\epsilon 1})$ and $C_{\epsilon(2x)} = C_{\epsilon 2} = C^I(\theta_{\epsilon 2})$, where $x \in \mathbb{Z}_+$ and $\epsilon = +\ (-)$ denotes a right (left) half line. For this QWHL, let us denote the eigenstate as

$$|\psi_\epsilon\rangle = \beta_{0,-\epsilon}\,|0,-\epsilon\rangle + \sum_{x\in\mathbb{Z}_+}\sum_{\delta'=\pm}\beta_{\epsilon x,\delta'}\,|\epsilon 2n,\delta'\rangle\,, \tag{A1}$$

where $\beta_{x,\delta} \in \mathbb{C}$. Substituting this eigenstate $|\psi_\epsilon\rangle$ into the eigenfunction, we have the equations of amplitudes as

$$\lambda_\epsilon\beta_{0,-\epsilon} = \beta_{0,-\epsilon}\omega_\epsilon(\epsilon s_{\epsilon 1}) + \beta_{\epsilon 1,\epsilon}(\epsilon s_{\epsilon 2})c_{\epsilon 1} + \beta_{\epsilon 1,-\epsilon}c_{\epsilon 2}c_{\epsilon 1}, \tag{A2}$$

$$\lambda_\epsilon\beta_{1,\epsilon} = \beta_{0,-\epsilon}\omega_\epsilon c_{\epsilon 1} - \beta_{\epsilon 1,\epsilon}(\epsilon s_{\epsilon 2})(\epsilon s_{\epsilon 1}) - \beta_{\epsilon 1,-\epsilon}c_{\epsilon 2}c_{\epsilon 1}, \tag{A3}$$

$$\lambda_\epsilon\beta_{\epsilon x,-\epsilon} = \beta_{\epsilon x,\epsilon}c_{\epsilon 2}(\epsilon s_{\epsilon 1}) - \beta_{\epsilon x,-\epsilon}(\epsilon s_{\epsilon 2})(\epsilon s_{\epsilon 1}) + \beta_{\epsilon(x+1),\epsilon}(\epsilon s_{\epsilon 2})c_{\epsilon 1} + \beta_{\epsilon(x+1),-\epsilon}c_{\epsilon 2}c_{\epsilon 1}, \tag{A4}$$

$$\lambda_\epsilon\beta_{\epsilon(x+1),\epsilon} = \beta_{\epsilon x,\epsilon}c_{\epsilon 2}c_{\epsilon 1} - \beta_{\epsilon x,-\epsilon}(\epsilon s_{\epsilon 2})c_{\epsilon 1} - \beta_{\epsilon(x+1),\epsilon}(\epsilon s_{\epsilon 2})(\epsilon s_{\epsilon 1}) - \beta_{\epsilon(x+1),-\epsilon}c_{\epsilon 2}(\epsilon s_{\epsilon 1}), \tag{A5}$$

where $s_{\epsilon x} = \sin\theta_{\epsilon x}$, $c_{\epsilon x} = \cos\theta_{\epsilon x}$, and λ_ϵ is the corresponding eigenvalue.

Multiplying Eqs. (A4) and (A5) by $c_{\epsilon 1}$ and $\epsilon s_{\epsilon 1}$, respectively, gives two new equations as

$$\lambda_\epsilon\beta_{\epsilon x,-\epsilon}c_{\epsilon 1} = \beta_{\epsilon x,\epsilon}c_{\epsilon 2}c_{\epsilon 1}(\epsilon s_{\epsilon 1}) - \beta_{\epsilon x,-\epsilon}(\epsilon s_{\epsilon 2})c_{\epsilon 1}(\epsilon s_{\epsilon 1}) + \beta_{\epsilon(x+1),\epsilon}(\epsilon s_{\epsilon 2})c_{\epsilon 1}^2 + \beta_{\epsilon(x+1),-\epsilon}c_{\epsilon 2}c_{\epsilon 1}^2,$$

$$\lambda_\epsilon\beta_{\epsilon(x+1),\epsilon}(\epsilon s_{\epsilon 1}) = \beta_{\epsilon x,\epsilon}c_{\epsilon 2}c_{\epsilon 1}(\epsilon s_{\epsilon 1}) - \beta_{\epsilon x,-\epsilon}(\epsilon s_{\epsilon 2})c_{\epsilon 1}(\epsilon s_{\epsilon 1}) - \beta_{\epsilon(x+1),\epsilon}(\epsilon s_{\epsilon 2})(\epsilon s_{\epsilon 1})^2 - \beta_{\epsilon(x+1),-\epsilon}c_{\epsilon 2}(\epsilon s_{\epsilon 1})^2.$$

Subtracting the second equation above from the first one and applying $c_{\epsilon 1}^2 + (\epsilon s_{\epsilon 1})^2 = 1$, the amplitude $\beta_{\epsilon x,\epsilon}$ is eliminated as

$$\beta_{\epsilon(x+1),\epsilon} = \frac{\lambda_\epsilon\beta_{\epsilon x,-\epsilon}c_{\epsilon 1} - \beta_{\epsilon(x+1),-\epsilon}c_{\epsilon 2}}{(\epsilon s_{\epsilon 2}) + \lambda_\epsilon(\epsilon s_{\epsilon 1})}. \tag{A6}$$

Similarly, multiplying Eqs. (A4) and (A5) by $\epsilon s_{\epsilon 1}$ and $c_{\epsilon 1}$, respectively, yields

$$\lambda_\epsilon\beta_{\epsilon x,-\epsilon}(\epsilon s_{\epsilon 1}) = \beta_{\epsilon x,\epsilon}c_{\epsilon 2}(\epsilon s_{\epsilon 1})^2 - \beta_{\epsilon x,-\epsilon}(\epsilon s_{\epsilon 2})(\epsilon s_{\epsilon 1})^2 + \beta_{\epsilon(x+1),\epsilon}(\epsilon s_{\epsilon 2})c_{\epsilon 1}(\epsilon s_{\epsilon 1}) + \beta_{\epsilon(x+1),-\epsilon}c_{\epsilon 2}c_{\epsilon 1}(\epsilon s_{\epsilon 1}),$$

$$\lambda_\epsilon\beta_{\epsilon(x+1),\epsilon}c_{\epsilon 1} = \beta_{\epsilon x,\epsilon}c_{\epsilon 2}c_{\epsilon 1}^2 - \beta_{\epsilon x,-\epsilon}(\epsilon s_{\epsilon 2})c_{\epsilon 1}^2 - \beta_{\epsilon(x+1),\epsilon}(\epsilon s_{\epsilon 2})c_{\epsilon 1}(\epsilon s_{\epsilon 1}) - \beta_{\epsilon(x+1),-\epsilon}c_{\epsilon 2}c_{\epsilon 1}(\epsilon s_{\epsilon 1}).$$

Adding the two equations above eliminates $\beta_{\epsilon(x+1),-\epsilon}$ as

$$\beta_{\epsilon x,-\epsilon} = \frac{\beta_{\epsilon x,\epsilon}c_{\epsilon 2} - \lambda_\epsilon\beta_{\epsilon(x+1),\epsilon}c_{\epsilon 1}}{\lambda_\epsilon(\epsilon s_{\epsilon 1}) + (\epsilon s_{\epsilon 2})}. \tag{A7}$$

Substituting Eq. (A7) into Eq. (A6), we have

$$\beta_{\epsilon(x+1),\epsilon} = \frac{\left(\lambda_\epsilon\beta_{\epsilon x,+}c_{\epsilon 2}c_{\epsilon 1} - \lambda_\epsilon^2\beta_{\epsilon(x+1),\epsilon}c_{\epsilon 1}^2 - \beta_{\epsilon(x+1),\epsilon}c_{\epsilon 2}^2 + \lambda_\epsilon\beta_{\epsilon(x+2),\epsilon}c_{\epsilon 2}c_{\epsilon 1}\right)}{[\lambda_\epsilon(\epsilon s_{\epsilon 1}) + (\epsilon s_{\epsilon 2})]^2}$$

$$\Rightarrow\left[1 + \lambda_\epsilon^2 + 2\lambda_\epsilon(\epsilon s_{\epsilon 1})(\epsilon s_{\epsilon 2})\right]\beta_{\epsilon(x+1),\epsilon} = c\lambda_\epsilon c_{\epsilon 2}c_{\epsilon 1}(\beta_{\epsilon x,+} + \beta_{\epsilon(x+2),\epsilon}), \tag{A8}$$

which is a recursive equation of $\beta_{\epsilon x,\epsilon}$ for $x \in \mathbb{Z}_+$.

The general solution of the recursive equation (A8) is $\beta_{\epsilon x,\epsilon} = Az^x + A'\frac{1}{z^x}$. Considering the convergence constraint $\lim_{x\to\infty}|\beta_{\epsilon x,\epsilon}| = 0$, the valid solution is of the form

$$\beta_{\epsilon x,\epsilon} = A_\epsilon z_\epsilon^x, \quad |z_\epsilon| < 1. \tag{A9}$$

Substituting this solution into Eq. (A8), we have

$$\begin{aligned}&\left[1+\lambda_\epsilon^2+2\lambda_\epsilon(\epsilon s_{\epsilon 1})(\epsilon s_{\epsilon 2})\right]A_\epsilon z_\epsilon^{x+1} = \lambda_\epsilon c_{\epsilon 2}c_{\epsilon 1}\left(A_\epsilon z_\epsilon^x + A_\epsilon z_\epsilon^{x+2}\right)\\ \Rightarrow&\left[1+\lambda_\epsilon^2+2\lambda_\epsilon(\epsilon s_{\epsilon 1})(\epsilon s_{\epsilon 2})\right]z_\epsilon = \lambda_\epsilon c_{\epsilon 2}c_{\epsilon 1}\left(1+z_\epsilon^2\right),\end{aligned} \tag{A10}$$

which is a equation of z_ϵ and λ_ϵ.

Other amplitudes can be obtained from Eq. (A9). Substituting Eq. (A9) into Eq. (A7) gives the amplitude

$$\beta_{\epsilon x,-} = \frac{c_{\epsilon 2}-\lambda_\epsilon c_{\epsilon 1}z_\epsilon}{\lambda_\epsilon(\epsilon s_{\epsilon 1})+(\epsilon s_{\epsilon 2})}A_\epsilon z_\epsilon^x. \tag{A11}$$

Multiplying Eqs. (A2) and (A3) by $(\epsilon s_{\epsilon 1})$ and $c_{\epsilon 1}$, respectively, gives

$$\begin{aligned}\lambda_\epsilon\beta_{0,-\epsilon}(\epsilon s_{\epsilon 1}) &= \beta_{0,-\epsilon}\omega_\epsilon(\epsilon s_{\epsilon 1})^2 + \beta_{\epsilon 1,\epsilon}(\epsilon s_{\epsilon 2})c_{\epsilon 1}(\epsilon s_{\epsilon 1}) + \beta_{\epsilon 1,-\epsilon}c_{\epsilon 2}c_{\epsilon 1}(\epsilon s_{\epsilon 1}),\\ \lambda_\epsilon\beta_{\epsilon 1,\epsilon}c_{\epsilon 1} &= \beta_{0,-\epsilon}\omega_\epsilon c_{\epsilon 1}^2 - \beta_{\epsilon 1,\epsilon}(\epsilon s_{\epsilon 2})c_{\epsilon 1}(\epsilon s_{\epsilon 1}) - \beta_{\epsilon 1,-\epsilon}c_{\epsilon 2}c_{\epsilon 1}(\epsilon s_{\epsilon 1}).\end{aligned}$$

Adding these two equations, the amplitude $\beta_{\epsilon 1,-\epsilon}$ is eliminated as

$$\lambda_\epsilon\beta_{0,-\epsilon}(\epsilon s_{\epsilon 1}) + \lambda_\epsilon\beta_{\epsilon 1,\epsilon}c_1 = \beta_{0,-\epsilon}\omega_\epsilon.$$

Substituting Eq. (A9) into the equation above gives the amplitude

$$\beta_{0,-\epsilon} = \frac{\lambda_\epsilon\beta_{\epsilon 1,\epsilon}c_{\epsilon 1}}{\omega_\epsilon-\lambda_\epsilon(\epsilon s_{\epsilon 1})} = \frac{\lambda_\epsilon c_{\epsilon 1}}{\omega_\epsilon-\lambda_\epsilon(\epsilon s_1)}Az. \tag{A12}$$

To obtain λ_ϵ and z_ϵ, we substitute the amplitudes in Eqs. (A9), (A11), and (A12) into Eq. (A3),

$$\begin{aligned}&[\lambda_\epsilon+(\epsilon s_{\epsilon 2})(\epsilon s_{\epsilon 1})]Az_\epsilon = \frac{\lambda_\epsilon c_{\epsilon 1}}{\omega_\epsilon-\lambda_\epsilon(\epsilon s_{\epsilon 1})}\omega_\epsilon c_{\epsilon 1}Az_\epsilon - \frac{c_{\epsilon 2}-\lambda_\epsilon c_{\epsilon 1}z_\epsilon}{\lambda_\epsilon(\epsilon s_{\epsilon 1})+(\epsilon s_{\epsilon 2})}c_{\epsilon 2}(\epsilon s_{\epsilon 1})Az_\epsilon\\
\Rightarrow&\lambda_\epsilon+(\epsilon s_{\epsilon 2})(\epsilon s_{\epsilon 1}) + \frac{c_{\epsilon 2}^2(\epsilon s_{\epsilon 1})-\lambda_\epsilon c_{\epsilon 2}c_{\epsilon 1}(\epsilon s_{\epsilon 1})z_\epsilon}{\lambda_\epsilon(\epsilon s_{\epsilon 1})+(\epsilon s_{\epsilon 2})} = \frac{\lambda_\epsilon\omega_\epsilon c_{\epsilon 1}^2}{\omega_\epsilon-\lambda_\epsilon(\epsilon s_{\epsilon 1})}\\
\Rightarrow&\frac{\lambda_\epsilon^2(\epsilon s_{\epsilon 1})+\lambda_\epsilon(\epsilon s_{\epsilon 2})+\lambda_\epsilon(\epsilon s_{\epsilon 2})(\epsilon s_{\epsilon 1})^2+(\epsilon s_{\epsilon 2})^2(\epsilon s_{\epsilon 1})+c_{\epsilon 2}^2(\epsilon s_{\epsilon 1})-\lambda_\epsilon c_{\epsilon 2}c_{\epsilon 1}(\epsilon s_{\epsilon 1})z_\epsilon}{\lambda_\epsilon(\epsilon s_{\epsilon 1})+(\epsilon s_{\epsilon 2})} = \frac{\lambda_\epsilon\omega_\epsilon c_{\epsilon 1}^2}{\omega_\epsilon-\lambda_\epsilon(\epsilon s_{\epsilon 1})}\\
\Rightarrow&\frac{(\epsilon s_{\epsilon 1})\left[\lambda_\epsilon^2+2\lambda_\epsilon(\epsilon s_{\epsilon 2})(\epsilon s_{\epsilon 1})+1\right]+\lambda_\epsilon(\epsilon s_{\epsilon 2})-\lambda_\epsilon(\epsilon s_{\epsilon 2})(\epsilon s_{\epsilon 1})^2-\lambda_\epsilon c_{\epsilon 2}c_{\epsilon 1}(\epsilon s_{\epsilon 1})z_\epsilon}{\lambda_\epsilon(\epsilon s_{\epsilon 1})+(\epsilon s_{\epsilon 2})} = \frac{\lambda_\epsilon\omega_\epsilon c_{\epsilon 1}^2}{\omega_\epsilon-\lambda_\epsilon(\epsilon s_{\epsilon 1})}\\
\Rightarrow&\frac{\lambda_\epsilon c_{\epsilon 2}c_{\epsilon 1}(\epsilon s_{\epsilon 1})\left(z_\epsilon+\frac{1}{z_\epsilon}\right)+\lambda_\epsilon(\epsilon s_{\epsilon 2})-\lambda_\epsilon(\epsilon s_{\epsilon 2})(\epsilon s_{\epsilon 1})^2-\lambda_\epsilon c_{\epsilon 2}c_{\epsilon 1}(\epsilon s_{\epsilon 1})z_\epsilon}{\lambda_\epsilon(\epsilon s_{\epsilon 1})+(\epsilon s_{\epsilon 2})} = \frac{\lambda_\epsilon\omega_\epsilon c_{\epsilon 1}^2}{\omega_\epsilon-\lambda_\epsilon(\epsilon s_{\epsilon 1})}\\
\Rightarrow&\frac{\lambda_\epsilon c_{\epsilon 2}c_{\epsilon 1}(\epsilon s_{\epsilon 1})\frac{1}{z_\epsilon}+\lambda_\epsilon(\epsilon s_{\epsilon 2})-\lambda_\epsilon(\epsilon s_{\epsilon 2})(\epsilon s_{\epsilon 1})^2}{\lambda_\epsilon(\epsilon s_{\epsilon 1})+(\epsilon s_{\epsilon 2})} = \frac{\lambda_\epsilon\omega_\epsilon c_{\epsilon 1}^2}{\omega_\epsilon-\lambda_\epsilon(\epsilon s_{\epsilon 1})}\\
\Rightarrow&\frac{\lambda_\epsilon c_{\epsilon 2}c_{\epsilon 1}(\epsilon s_{\epsilon 1})\frac{1}{z_\epsilon}+\lambda_\epsilon(\epsilon s_{\epsilon 2})c_{\epsilon 1}^2}{\lambda_\epsilon(\epsilon s_{\epsilon 1})+(\epsilon s_{\epsilon 2})} = \frac{\lambda_\epsilon\omega_\epsilon c_{\epsilon 1}^2}{\omega_\epsilon-\lambda_\epsilon(\epsilon s_{\epsilon 1})}\\
\Rightarrow&\frac{c_{\epsilon 2}(\epsilon s_{\epsilon 1})\frac{1}{z_\epsilon}+(\epsilon s_{\epsilon 2})c_{\epsilon 1}}{\lambda_\epsilon(\epsilon s_{\epsilon 1})+(\epsilon s_{\epsilon 2})} = \frac{\omega_\epsilon c_{\epsilon 1}}{\omega_\epsilon-\lambda_\epsilon(\epsilon s_{\epsilon 1})}\\
\Rightarrow&\frac{1}{z_\epsilon} = \frac{1}{c_{\epsilon 2}(\epsilon s_{\epsilon 1})}\frac{\lambda_\epsilon c_{\epsilon 1}(\epsilon s_{\epsilon 1})[\omega_\epsilon+(\epsilon s_{\epsilon 2})]}{\omega_\epsilon-\lambda_\epsilon(\epsilon s_{\epsilon 1})} = \frac{\lambda_\epsilon c_{\epsilon 1}[\omega_\epsilon+(\epsilon s_{\epsilon 2})]}{c_{\epsilon 2}[\omega_\epsilon-\lambda_\epsilon(\epsilon s_{\epsilon 1})]},\end{aligned}$$

where the fifth line is due to Eq. (A10). Hence, for each eigenvalue λ_ϵ, the parameter z_ϵ is determined by

$$z_\epsilon = \frac{c_{\epsilon 2}[\omega_\epsilon-\lambda_\epsilon(\epsilon s_{\epsilon 1})]}{\lambda_\epsilon c_{\epsilon 1}[\omega_\epsilon+(\epsilon s_{\epsilon 2})]}. \tag{A13}$$

Substituting Eq. (A13) into the equation of λ_ϵ and z_ϵ in Eq. (A10), we have

$$\big[1+\lambda_\epsilon^2+2\lambda_\epsilon(\epsilon s_{\epsilon 1})(\epsilon s_{\epsilon 2})\big]\frac{c_{\epsilon 2}[\omega_\epsilon-\lambda_\epsilon(\epsilon s_{\epsilon 1})]}{\lambda_\epsilon c_{\epsilon 1}[\omega_\epsilon+(\epsilon s_{\epsilon 2})]}=\lambda_\epsilon c_{\epsilon 2}c_{\epsilon 1}\left(1+\frac{c_{\epsilon 2}^2[\omega_\epsilon-\lambda_\epsilon(\epsilon s_{\epsilon 1})]^2}{\lambda_\epsilon^2 c_{\epsilon 1}^2[\omega_\epsilon+(\epsilon s_{\epsilon 2})]^2}\right)$$
$$\Rightarrow\big[1+\lambda_\epsilon^2+2\lambda_\epsilon(\epsilon s_{\epsilon 1})(\epsilon s_{\epsilon 2})\big][\omega_\epsilon+(\epsilon s_{\epsilon 2})][\omega_\epsilon-\lambda_\epsilon(\epsilon s_{\epsilon 1})]=\lambda_\epsilon^2 c_{\epsilon 1}^2[\omega_\epsilon+(\epsilon s_{\epsilon 2})]^2+c_{\epsilon 2}^2[\omega_\epsilon-\lambda_\epsilon(\epsilon s_{\epsilon 1})]^2$$
$$\Rightarrow-[\lambda_\epsilon(\epsilon s_{\epsilon 1})+(\epsilon s_{\epsilon 2})]\big\{[\omega_\epsilon+(\epsilon s_{\epsilon 2})]\lambda_\epsilon^2-(\epsilon s_{\epsilon 1})\big(\omega_\epsilon^2-1\big)\lambda_\epsilon-\big[\omega_\epsilon^2(\epsilon s_{\epsilon 2})+\omega_\epsilon\big]\big\}=0.$$

A solution of the above equation is $\lambda=-\frac{s_{\epsilon 2}}{s_{\epsilon 1}}$, which leads to $\lambda_\epsilon(\epsilon s_{\epsilon 1})+(\epsilon s_{\epsilon 2})=0$. However, this solution satisfies $|\lambda_\epsilon|=1$ only when $s_{\epsilon 2}=\pm s_{\epsilon 1}$, with which we have $|z_\epsilon|=1\not<1$. Therefore, the eigenvalue is a solution of the quadratic equation

$$[\omega_\epsilon+(\epsilon s_{\epsilon 2})]\lambda_\epsilon^2-(\epsilon s_{\epsilon 1})\big(\omega_\epsilon^2-1\big)\lambda_\epsilon-\big[\omega_\epsilon^2(\epsilon s_{\epsilon 2})+\omega_\epsilon\big]=0,$$

which can be easily solved as

$$\lambda_\epsilon^\varepsilon=\frac{(\epsilon s_{\epsilon 1})\big(\omega_\epsilon^2-1\big)+\varepsilon\sqrt{(\epsilon s_{\epsilon 1})^2\big(\omega_\epsilon^2-1\big)^2+4[\omega_\epsilon+(\epsilon s_{\epsilon 2})]\big[\omega_\epsilon^2(\epsilon s_{\epsilon 2})+\omega_\epsilon\big]}}{2[\omega_\epsilon+(\epsilon s_{\epsilon 2})]},\tag{A14}$$

where $\varepsilon=\pm$ comes from the quadratic formula.

After obtaining λ_ϵ, the parameter z_ϵ can be determined according to Eq. (A13). After that, all amplitudes can be obtained via Eqs. (A9), (A11), and (A12), where the normalization factor A can be easily obtained using the sum of a geometric series as

$$A=1\Bigg/\sqrt{\frac{|z_\epsilon|^2}{1-|z_\epsilon|^2}\left(1+\left|\frac{c_{\epsilon 2}-c_{\epsilon 1}\lambda z_\epsilon}{\epsilon s_{\epsilon 2}+\epsilon s_{\epsilon 1}\lambda}\right|^2\right)+\left|\frac{c_{\epsilon 1}\lambda}{\omega-\epsilon s_{\epsilon 1}\lambda}\right|^2|z_\epsilon|^2}.\tag{A15}$$

In addition, it can be shown that the eigenvalue in Eq. (A14) always satisfies $|\lambda_\epsilon^\varepsilon|^2=1$. To this end, we further deduce λ_ϵ as

$$\begin{aligned}\lambda_\epsilon&=\frac{(\epsilon s_{\epsilon 1})\big(\omega_\epsilon^2-1\big)\pm\sqrt{(\epsilon s_{\epsilon 1})^2\big(\omega_\epsilon^2-1\big)^2+4[\omega_\epsilon+(\epsilon s_{\epsilon 2})]\big[\omega_\epsilon^2(\epsilon s_{\epsilon 2})+\omega_\epsilon\big]}}{2[\omega_\epsilon+(\epsilon s_{\epsilon 2})]}\\
&=\frac{(\epsilon s_{\epsilon 1})\omega_\epsilon(\omega_\epsilon-\omega_\epsilon^*)\pm\sqrt{s_{\epsilon 1}^2\omega_\epsilon^2(\omega_\epsilon-\omega_\epsilon^*)^2+4\omega_\epsilon^2[\omega_\epsilon+(\epsilon s_{\epsilon 2})][(\epsilon s_{\epsilon 2})+\omega_\epsilon^*]}}{2\omega_\epsilon[1+(\epsilon s_{\epsilon 2})\omega_\epsilon^*]}\\
&=\frac{(\epsilon s_{\epsilon 1})(2i\mathrm{Im}[\omega_\epsilon])\pm\sqrt{s_{\epsilon 1}^2(2i\mathrm{Im}[\omega_\epsilon])^2+4\big[1+s_{\epsilon 2}^2+(\epsilon s_{\epsilon 2})\omega_\epsilon^*+(\epsilon s_{\epsilon 2})\omega_\epsilon\big]}}{2[1+(\epsilon s_{\epsilon 2})\omega_\epsilon^*]}\\
&=\frac{(\epsilon s_{\epsilon 1})(i\mathrm{Im}[\omega_\epsilon])\pm\sqrt{-s_{\epsilon 1}^2\mathrm{Im}[\omega_\epsilon]^2+\big[1+s_{\epsilon 2}^2+(\epsilon s_{\epsilon 2})\omega_\epsilon^*+(\epsilon s_{\epsilon 2})\omega_\epsilon\big]}}{[1+(\epsilon s_{\epsilon 2})\omega_\epsilon^*]}\\
&=\frac{(\epsilon s_{\epsilon 1})(i\mathrm{Im}[\omega_\epsilon])\pm\sqrt{-s_{\epsilon 1}^2\mathrm{Im}[\omega_\epsilon]^2+1+s_{\epsilon 2}^2+2(\epsilon s_{\epsilon 2})\mathrm{Re}[\omega_\epsilon]}}{[1+(\epsilon s_{\epsilon 2})\omega_\epsilon^*]}\\
&=\frac{(\epsilon s_{\epsilon 1})(i\mathrm{Im}[\omega_\epsilon])\pm\sqrt{-s_{\epsilon 1}^2\mathrm{Im}[\omega_\epsilon]^2+\mathrm{Im}[\omega_\epsilon]^2+\mathrm{Re}[\omega_\epsilon]^2+s_{\epsilon 2}^2+2(\epsilon s_{\epsilon 2})\mathrm{Re}[\omega_\epsilon]}}{[1+(\epsilon s_{\epsilon 2})\omega_\epsilon^*]}\\
&=\frac{(\epsilon s_{\epsilon 1})(i\mathrm{Im}[\omega_\epsilon])\pm\sqrt{(1-s_{\epsilon 1}^2)\mathrm{Im}[\omega_\epsilon]^2+\{\mathrm{Re}[\omega_\epsilon]+(\epsilon s_{\epsilon 2})\}^2}}{[1+(\epsilon s_{\epsilon 2})\omega_\epsilon^*]}.\end{aligned}$$

It is easy to see that the term $\sqrt{(1-s_{\epsilon 1}^2)\mathrm{Im}[\omega_\epsilon]^2+\{\mathrm{Re}[\omega_\epsilon]+(\epsilon s_{\epsilon 2})\}^2}$ is real. Therefore, we have

$$\begin{aligned}|\lambda_\epsilon|^2&=\frac{s_{\epsilon 1}^2\mathrm{Im}[\omega_\epsilon]^2+\big(1-s_{\epsilon 1}^2\big)\mathrm{Im}[\omega_\epsilon]^2+\{\mathrm{Re}[\omega_\epsilon]+(\epsilon s_{\epsilon 2})\}^2}{\big[1+(\epsilon s_{\epsilon 2})\omega_\epsilon^*\big][1+(\epsilon s_{\epsilon 2})\omega_\epsilon]}\\
&=\frac{\mathrm{Im}[\omega_\epsilon]^2+\mathrm{Re}[\omega_\epsilon]^2+s_{\epsilon 2}^2+2(\epsilon s_{\epsilon 2})\mathrm{Re}[\omega_\epsilon]}{1+s_{\epsilon 2}^2+2(\epsilon s_{\epsilon 2})\mathrm{Re}[\omega_\epsilon]}\\
&=1.\end{aligned}$$

[1] A. M. Childs, Phys. Rev. Lett. **102**, 180501 (2009).
[2] A. M. Childs, D. Gosset, and Z. Webb, Science **339**, 791 (2013).
[3] G. Di Molfetta, M. Brachet, and F. Debbasch, Phys. Rev. A **88**, 042301 (2013).
[4] W.-W. Zhang, S. K. Goyal, F. Gao, B. C. Sanders, and C. Simon, New J. Phys. **18**, 093025 (2016).
[5] W.-W. Zhang, S. K. Goyal, C. Simon, and B. C. Sanders, Phys. Rev. A **95**, 052351 (2017).
[6] N. C. Harris, G. R. Steinbrecher, M. Prabhu, Y. Lahini, J. Mower, D. Bunandar, C. Chen, F. N. C. Wong, T. Baehr-Jones, M. Hochberg, S. Lloyd, and D. Englund, Nat. Photon. **11**, 447 (2017).
[7] M. Sajid, J. K. Asbóth, D. Meschede, R. F. Werner, and A. Alberti, Phys. Rev. B **99**, 214303 (2019).
[8] Z. Yan, Y.-R. Zhang, M. Gong, Y. Wu, Y. Zheng, S. Li, C. Wang, F. Liang, J. Lin, Y. Xu, C. Guo, L. Sun, C.-Z. Peng, K. Xia, H. Deng, H. Rong, J. Q. You, F. Nori, H. Fan, X. Zhu *et al.*, Science **364**, 753 (2019).
[9] K. Wang, X. Qiu, L. Xiao, X. Zhan, Z. Bian, B. C. Sanders, W. Yi, and P. Xue, Nat. Commun. **10**, 2293 (2019).
[10] S. Panahiyan and S. Fritzsche, Phys. Rev. A **103**, 012201 (2021).
[11] Y. Aharonov, L. Davidovich, and N. Zagury, Phys. Rev. A **48**, 1687 (1993).
[12] J. Kempe, Contemp. Phys. **44**, 307 (2003).
[13] R. Portugal, *Quantum Walks and Search Algorithms* (Springer, New York, 2013), Vol. 19.
[14] A. Montanaro, npj Quantum Inf. **2**, 15023 (2016).
[15] N. Shenvi, J. Kempe, and K. Birgitta Whaley, Phys. Rev. A **67**, 052307 (2003).
[16] J. A. Izaac, X. Zhan, Z. Bian, K. Wang, J. Li, J. B. Wang, and P. Xue, Phys. Rev. A **95**, 032318 (2017).
[17] Y. Xu, D. Zhang, and L. Li, Phys. Rev. A **106**, 052207 (2022).
[18] W. Zhou, J. Phys.: Conf. Ser. **1748**, 032022 (2021).
[19] N. Inui, Y. Konishi, and N. Konno, Phys. Rev. A **69**, 052323 (2004).
[20] Y. Shikano and H. Katsura, Phys. Rev. E **82**, 031122 (2010).
[21] B. Kollár, M. Štefaňák, T. Kiss, and I. Jex, Phys. Rev. A **82**, 012303 (2010).
[22] X. Zhan, H. Qin, Z.-H. Bian, J. Li, and P. Xue, Phys. Rev. A **90**, 012331 (2014).
[23] P. Xue, R. Zhang, H. Qin, X. Zhan, Z. H. Bian, J. Li, and B. C. Sanders, Phys. Rev. Lett. **114**, 140502 (2015).
[24] S. Dadras, A. Gresch, C. Groiseau, S. Wimberger, and G. S. Summy, Phys. Rev. Lett. **121**, 070402 (2018).
[25] B. Wang, T. Chen, and X. Zhang, Phys. Rev. Lett. **121**, 100501 (2018).
[26] D. Xie, T.-S. Deng, T. Xiao, W. Gou, T. Chen, W. Yi, and B. Yan, Phys. Rev. Lett. **124**, 050502 (2020).
[27] Y. F. Peng, W. Wang, and X. X. Yi, Phys. Rev. A **103**, 032205 (2021).
[28] B. Danacı, I. Yalçınkaya, B. Çakmak, G. Karpat, S. P. Kelly, and A. L. Subaşı, Phys. Rev. A **103**, 022416 (2021).
[29] J. Ghosh, Phys. Rev. A **89**, 022309 (2014).
[30] H. T. Lam, Y. Yu, and K. Y. Szeto, Phys. Rev. A **93**, 052319 (2016).
[31] C. Chen, X. Ding, J. Qin, Y. He, Y.-H. Luo, M.-C. Chen, C. Liu, X.-L. Wang, W.-J. Zhang, H. Li, L.-X. You, Z. Wang, D.-W. Wang, B. C. Sanders, C.-Y. Lu, and J.-W. Pan, Phys. Rev. Lett. **121**, 100502 (2018).
[32] L. Xiao, X. Zhan, Z. H. Bian, K. K. Wang, X. Zhang, X. P. Wang, J. Li, K. Mochizuki, D. Kim, N. Kawakami, W. Yi, H. Obuse, B. C. Sanders, and P. Xue, Nat. Phys. **13**, 1117 (2017).
[33] L. Xiao, K. Wang, X. Zhan, Z. Bian, K. Kawabata, M. Ueda, W. Yi, and P. Xue, Phys. Rev. Lett. **123**, 230401 (2019).
[34] H. Tang, T.-Y. Wang, Z.-Y. Shi, Z. Feng, Y. Wang, X.-W. Shang, J. Gao, Z.-Q. Jiao, Z.-M. Li, Y.-J. Chang, W.-H. Zhou, Y.-H. Lu, Y.-L. Yang, R.-J. Ren, L.-F. Qiao, and X.-M. Jin, Photon. Res. **10**, 1430 (2022).
[35] C. M. Chandrashekar, Phys. Rev. A **83**, 022320 (2011).
[36] C. Cedzich and A. H. Werner, Commun. Math. Phys. **387**, 1257 (2021).
[37] J. Wu, W.-W. Zhang, and B. C. Sanders, Front. Phys. **14**, 61301 (2019).
[38] J. K. Asbóth, Phys. Rev. B **86**, 195414 (2012).
[39] H. Obuse, J. K. Asbóth, Y. Nishimura, and N. Kawakami, Phys. Rev. B **92**, 045424 (2015).
[40] J. K. Asbóth and H. Obuse, Phys. Rev. B **88**, 121406(R) (2013).
[41] T. Nitsche, T. Geib, C. Stahl, L. Lorz, C. Cedzich, S. Barkhofen, R. F. Werner, and C. Silberhorn, New J. Phys. **21**, 043031 (2019).
[42] T. Kitagawa, M. A. Broome, A. Fedrizzi, M. S. Rudner, E. Berg, I. Kassal, A. Aspuru-Guzik, E. Demler, and A. G. White, Nat. Commun. **3**, 882 (2012).
[43] C. Cedzich, F. A. Grünbaum, C. Stahl, L. Velázquez, A. H. Werner, and R. F. Werner, J. Phys. A: Math. Theor. **49**, 21LT01 (2016).
[44] T. Kitagawa, M. S. Rudner, E. Berg, and E. Demler, Phys. Rev. A **82**, 033429 (2010).
[45] T. Kitagawa, Quantum Inf. Proc. **11**, 1107 (2012).
[46] A. Grudka, M. Karczewski, P. Kurzyński, J. Wójcik, and A. Wójcik, Phys. Rev. A **107**, 032201 (2023).
[47] P. W. Anderson, Phys. Rev. **109**, 1492 (1958).
[48] A. Ahlbrecht, V. B. Scholz, and A. H. Werner, J. Math. Phys. **52**, 102201 (2011).
[49] A. Schreiber, K. N. Cassemiro, V. Potoček, A. Gábris, I. Jex, and C. Silberhorn, Phys. Rev. Lett. **106**, 180403 (2011).
[50] J. M. Edge and J. K. Asboth, Phys. Rev. B **91**, 104202 (2015).
[51] T. Rakovszky and J. K. Asboth, Phys. Rev. A **92**, 052311 (2015).
[52] C. V. C. Mendes, G. M. A. Almeida, M. L. Lyra, and F. A. B. F. de Moura, Phys. Rev. E **99**, 022117 (2019).
[53] S. De, D. Bagrets, K. W. Kim, S. Barkhofen, J. Sperling, B. Brecht, A. Altland, T. Micklitz, and C. Silberhorn, Topological anderson localization transition in time-multiplexed quantum walks, in *2021 Conference on Lasers and Electro-Optics Europe & European Quantum Electronics Conference (CLEO/Europe-EQEC)* (Munich, Germany, 2021), pp. 1-1.
[54] D. Bagrets, K. W. Kim, S. Barkhofen, S. De, J. Sperling, C. Silberhorn, A. Altland, and T. Micklitz, Phys. Rev. Res. **3**, 023183 (2021).
[55] X. Zhan, L. Xiao, Z. Bian, K. Wang, X. Qiu, B. C. Sanders, W. Yi, and P. Xue, Phys. Rev. Lett. **119**, 130501 (2017).
[56] M. J. Cantero, F. A. Grunbaum, L. Moral, and L. Velazquez, One-dimensional quantum walks with one defect, arXiv:1010.5762.
[57] M. J. Cantero, F. Grünbaum, L. Moral, and L. Velázquez, Rev. Math. Phys. **24**, 1250002 (2012).

[58] A. Wójcik, T. Łuczak, P. Kurzyński, A. Grudka, T. Gdala, and M. Bednarska-Bzdęga, Phys. Rev. A **85**, 012329 (2012).
[59] R. Zhang, P. Xue, and J. Twamley, Phys. Rev. A **89**, 042317 (2014).
[60] T. Fuda, D. Funakawa, and A. Suzuki, Quantum Inf. Proc. **16**, 203 (2017).
[61] N. Konno and E. Segawa, Quantum Inf. Comput. **11**, 0485 (2011).